

Soft Matter

Accepted Manuscript



This is an *Accepted Manuscript*, which has been through the Royal Society of Chemistry peer review process and has been accepted for publication.

Accepted Manuscripts are published online shortly after acceptance, before technical editing, formatting and proof reading. Using this free service, authors can make their results available to the community, in citable form, before we publish the edited article. We will replace this *Accepted Manuscript* with the edited and formatted *Advance Article* as soon as it is available.

You can find more information about *Accepted Manuscripts* in the [Information for Authors](#).

Please note that technical editing may introduce minor changes to the text and/or graphics, which may alter content. The journal's standard [Terms & Conditions](#) and the [Ethical guidelines](#) still apply. In no event shall the Royal Society of Chemistry be held responsible for any errors or omissions in this *Accepted Manuscript* or any consequences arising from the use of any information it contains.

Table of Contents only:

Surface Structure of Poly(methyl methacrylate) Films Influenced by Chain Entanglement in the Corresponding Film-Formation Solution

Jianquan Xu, Yinjun Liu, Jinsheng He, RongPing Zhang, Biao Zuo, Xinping Wang*



Surface structure of poly(methyl methacrylate) films influenced by chain entanglement in the corresponding film-formation solution

Surface Structure of Poly(methyl methacrylate) Films Influenced by Chain Entanglement in the Corresponding Film-Formation Solution

Jianquan Xu, Yinjun Liu, Jinsheng He, Rongping Zhang, Biao Zuo, Xinping Wang*

Department of Chemistry, Key Laboratory of Advanced Textile Materials and Manufacturing Technology of the Education Ministry, Zhejiang Sci-Tech University, Hangzhou 310018, China

ABSTRACT: The effects of the properties of casting solution on the surface structure of poly(methyl methacrylate) (PMMA) films were systematically investigated. It was observed that the hydrophobicity of PMMA films increased with increasing viscosity of the corresponding polymer solution regardless of the film-forming techniques that were utilized. The ratio of the C-H symmetric stretching vibrations of methylene groups (hydrophobic component, with peak at 2910 cm^{-1}) to that of the ester methyl groups (relative hydrophilic component, with peak at 2955 cm^{-1}) from sum frequency generation (SFG) vibrational spectra, A_{2910}/A_{2955} , was used as a parameter to evaluate the structure on the film surface, which was related to the surface wettability of the films. The results showed that A_{2910}/A_{2955} of cast PMMA films increased linearly with $\eta_{sp}^{0.3}$ (η_{sp} , the specific viscosity of the casting solution), whereas that of the corresponding spin-coated films showed a linear relationship defined as $\eta_{sp}^{0.3}E^{0.26}$, where E is the average number of entanglement points per molecule ($E = M_w/M_e$). These results indicate that a relative equilibrium conformation on the PMMA film surface, adopted from the perspective of thermodynamics, was easily achieved during film formation, when the

conformation of the polymer chains in the corresponding casting solution was close to that in the bulk. For the spin-coated films, the chain entanglement structure in the casting solution was a more important factor for the resulting film to reach a relative equilibrium state, since this structure was in favor of maintaining pristine conformation in casting solution under centrifugal force during spin-coating. This work may help to enhance the fundamental understanding of the formation of film surface structure from polymer solution to the resulting solid film, which will affect not only the corresponding surface properties, but also the dynamics of the resulting thin films.

Keywords: surface structure; PMMA film; polymer solution; viscosity; entanglement

1. INTRODUCTION

Thin polymer films have been used in a wide variety of applications, such as microelectronics, lithography, selective membranes, organic sensors and devices, and protective coatings.¹⁻⁴ Spin coating is widely employed to fabricate polymer thin films over large areas with high structural uniformity and specific thickness. Changing the solution viscosity via the concentration or molecular weight, allows the thickness of the resulting film to be precisely controlled from a thickness of a few nanometers to sub-micrometers.^{5,6} The spinning rate, of course, also controls the thickness. This easy, quick and inexpensive method has been adopted not only in laboratories in academia, but also on an industrial scale in factories. A general problem of this method is that the polymer chains adopt an elongated conformation in the substrate plane due to the torque caused by the spinning and the rapid solvent evaporation, and they are eventually frozen out and are far from being in a quasi-equilibrium state in the resulting film.⁶⁻¹⁰

Another commonly used film-forming method, solution casting, is a much milder process, which involves leaving the polymer solution placed on a flat substrate to

evaporate slowly. Properties such as crystallinity, chain packing, and orientation can differ for films prepared from different film-forming methods.¹¹⁻²¹ Wong²¹ observed that the chain conformation of poly(3-hexylthiophene) spin-coated films were the furthest from equilibrium, while solution casting produced films that were the most isotropic. Lu^{16,18} demonstrated that the main chain of a polymer will orient along the substrate plane when the spin-coated polymer and the substrate can wet each other, while no orientation was found for solution-cast films. It was reported¹⁹ that the emission color and quantum efficiency of MEH-PPV LEDs could be controlled by simply adjusting the spin-casting conditions, suggesting that thin film preparation is a much more complicated process than previously assumed. Significant in-plane optical anisotropy was observed for both the real and the imaginary parts of the transmittance of poly (2,5-pyridine diyl) films, which is a result of the partial alignment of the polymer chains, oriented radially outward from the center of the film during the spin-casting process.⁴

The structure of the outermost layer is of great significance in determining the surface properties of thin polymer films, such as wettability, adhesion, and friction. Due to the complexity of the film-forming process, the relationship between the surface molecular structure of polymer thin films and the film-forming methods have been little studied and are accordingly not clearly understood.^{7-18, 20-24} In general, the surface structure formation is governed by thermodynamics, but the kinetics for the segregation and array processes are mainly determined by fixed process methods and conditions which also play an important role in the ultimate surface structure formation. do Rego²² investigated the surface composition of PS-b-PEO copolymer films and found that the amount of surface polystyrene for the non-annealed solution-cast films was higher than that of spin-coated films. Recently, our group demonstrated the relationship between solution properties, film-forming methods, and the surface structure of random fluorinated copolymer films.^{14,23,24} It was observed that when entropic forces dominated the solution–air interfacial structure, film preparation by spin-coating weakened the entropy effect of the polymer chains due to centrifugal force, resulting in the segregation of the fluorinated moieties on the film

surface. When the migration of perfluoroalkyl groups at the solution–air interface was controlled by enthalpic forces, the segregation extent of the perfluoroalkyl groups at the surface of the film was determined by the solidification time of the polymer solution. Tanaka¹⁷ studied the local conformation of polystyrene chains on silicon substrates by SFG combined with dissipative particle dynamics simulations and found that the chains adopted an elongated conformation in the substrate plane induced by the spinning torque or the centrifugal force during the spin-coating process, while no interfacial orientation of chains was observed for the PS films when prepared by the solution-casting method.

In addition, there has been enormous interest in the question of how surface and its size affect the glass transition temperature of thin polymer films. Different groups of researchers have reached conflicting conclusions to this question during the last 20 years, even when studying the same type of polymer. In the last few years, there has been some evidence that this controversy is due to the fact that the equilibration of thin polymeric films on substrates is not sufficiently well controlled (and not well understood). According to the layer model^{25,26}, the structure on a surface layer plays an important role in the glass transition behavior of the corresponding thin polymer film. Therefore, there is need for a careful examination of the factors which control the establishment of thermal equilibrium in such polymer films when various film-formation methods and properties of casting solution are applied. At the same time, it is also necessary to understand the effect of film formation conditions on the surface structure of the resulting films.

In this paper, the surface structures of thin PMMA films prepared by various conditions, including different film-formation methods, casting solution concentrations and PMMA molecular weights, were investigated by contact angle goniometry and sum frequency spectroscopy (SFG), which can provide abundant information about the molecular structure on the film surfaces. The aim of this work is to systematically investigate the influence of the film-forming methods and casting solution properties on the corresponding surface structure of PMMA films. This may help to enhance the fundamental understanding of the formation of film surface

structures from polymer solution to the resulting solid film.

2. EXPERIMENTAL SECTION

2.1. Materials

Poly(methyl methacrylate) (PMMA) samples with different molecular weights were synthesized by the ATRP technique as reported previously.^{27,28} The molecular weights and polydispersity index (PDI) of the polymers were determined by gel permeation chromatography (GPC) using a Waters 1500 GPC apparatus (with THF as the eluent at a flow rate of 1.0mL/min). The GPC chromatograms were calibrated against polystyrene standards. The tacticity of PMMA calculated from ¹H-NMR spectra were recorded on a Bruker Avance AMX-400 NMR spectrometer in CDCl₃ with tetramethylsilane (TMS) as the internal standard. The characteristics of the PMMA samples used in this study are shown in Table 1. Toluene was purchased from Shanghai Reagent Co. and used without further purification. Fused silica was used as substrates. The substrates were cleaned before use in a piranha solution (a mixture of H₂SO₄ and H₂O₂ in 3:1 by volume) at 90°C for 20 min and then thoroughly rinsed in deionized water and dried in pure nitrogen gas.

Table 1. Characteristics of the PMMA used in this study

Sample	M_n ^{a)}	PDI ^{a)}	mm ^{b)}	mr ^{b)}	rr ^{b)}
M232	23200	1.13	0.05	0.36	0.59
M540	55740	1.12	0.05	0.35	0.60
M1027	107100	1.09	0.04	0.36	0.60

a) determined by GPC; b) obtained from ¹H NMR spectra

2.2 Film Preparation

The PMMA solutions of various concentrations were prepared by dissolving different amounts of polymer in toluene, which were then filtered through a porous sand core filter with pore size of 0.25 μm in diameter. Two film-forming techniques, spin-coating and solution-casting, were employed to prepare thin PMMA films on the

clean fused silica. Both types of films were first dried in air for 24 h and then in vacuum at room temperature for another 48h. The films obtained by solution-casting were denoted “cast”, and their spin-coated counterparts were denoted “spin”.

2.3. Characterization

Contact angles (θ) were measured by the Sessile drop method at room temperature and ambient humidity with a Krüss (Hamburg, Germany) DSA-10 contact angle goniometer. The reported θ values were the averages of at least eight measurements taken within 5 seconds of applying each drop of liquid. The experimental errors when measuring the θ values were evaluated to be less than $\pm 2^\circ$, thus indicating that the results were sufficiently accurate. Contact angles of water and diiodomethane were used to make estimates of the surface free energy for various samples according to the theory of Owens and Wendt.²⁹

Atomic force microscopy (XEI-100, SPM, PSIA Co.) was used to investigate the morphology of the top surface of the samples. SPM measurements were performed in air with an etched silicon probe having a length of 125 μm . Scanning was carried out in the tapping mode at a frequency of approximately 300 Hz.

Viscosities of polymer solutions were conveniently measured using Ubbelohde-type capillary viscometers at 25 ± 0.02 °C. The measured viscosity of the solution was then divided by the viscosity of the solvent to obtain the relative viscosity, η_r . The specific viscosity, determined as $\eta_{sp} = \eta_r - 1$, expresses the incremental viscosity attributable to the polymeric solute.

2.5. Sum-Frequency Generation Spectroscopy

Sum frequency generation (SFG) vibrational spectra were obtained using a custom-designed EKSPLA SFG spectrometer that has been described in detail by various researchers.³⁰⁻³² Briefly, the visible input beam at 0.532 μm was generated by frequency doubling of part of the fundamental output from an EKSPLA Nd: YAG laser. The IR beam, tunable between 1000 and 4300 cm^{-1} (with a line width $<6\text{cm}^{-1}$), was obtained from an optical parametric generation/amplification/difference frequency generation (OPG/OPA/ DFG) system based on LBO and AgGaS₂ crystals.

Both beams were pumped by the second harmonic and the fundamental output of the laser and had a pulse width of ~30 ps, a repetition rate of 50 Hz, and a typical beam diameter of 0.5 mm at the sample surface or interface. The incident angles of the visible beam and the IR beam were 60° and 55°, respectively, with respective energies at the sample surface of ~230 and ~130 μJ. The measurements were carried out at room temperature using two types of polarization combinations, namely *ssp* and *ppp* (SF output, visible input, and infrared input). In the SFG spectra presented below, each data point represents an average of 500 laser shots of five individual experiments, and the standard deviation for each data point is less than ± 3%.

The intensity of the sum frequency signal can be expressed as follows:³³

$$I_{SFG} \propto \left| \chi_{eff}^{(2)} \right|^2 \cdot I_{vis} \cdot I_{IR} \quad (1)$$

Where I_{vis} and I_{IR} are the intensities of the two input lasers (visible and infrared, respectively), and $\chi_{eff}^{(2)}$ is the effective nonlinear susceptibility, which can be expressed in the form:

$$\chi_{eff}^{(2)} = \chi_{NR}^{(2)} + \chi_R^{(2)} = \chi_{NR}^{(2)} + \sum_q \frac{A_q}{\omega_{IR} - \omega_q + i\Gamma_q} \quad (2)$$

Where $\chi_{NR}^{(2)}$ is the nonresonant contribution and $\chi_R^{(2)}$ is the resonant contribution. $\chi_R^{(2)}$ consists of A_q , ω_{IR} , ω_q , and Γ_q , which are the strength, the frequency of the incoming IR beam, the resonant frequency, and damping coefficient of the q th resonant vibrational mode, respectively. A_q was determined from equations (1) and (2) by performing Lorentzian fits to the experimental data.

3. RESULTS AND DISCUSSION

3.1 The surface wettability and structure of PMMA films prepared by different film-forming methods.

Contact angle measurement is one of the most effective and sensitive methods for characterizing polymer surface structure, by which subtle changes in polymer surface properties can be detected.³⁴⁻³⁶ The water contact angles and the surface free energies of PMMA films prepared by spin-coating and solution casting are presented in Fig. 1.

The water contact angles of both spin-coated and cast films were about 70° and 88° respectively. According to the theory of Owens and Wendt,²⁹ the surface free energy of the spin-coated film was estimated to be 49 mJ/m^2 , whereas that of the corresponding cast film was 43 mJ/m^2 . In these cases, the surface of the spin-coated film possesses a relatively hydrophilic surface, as well as a higher surface energy, compared to the corresponding cast sample.

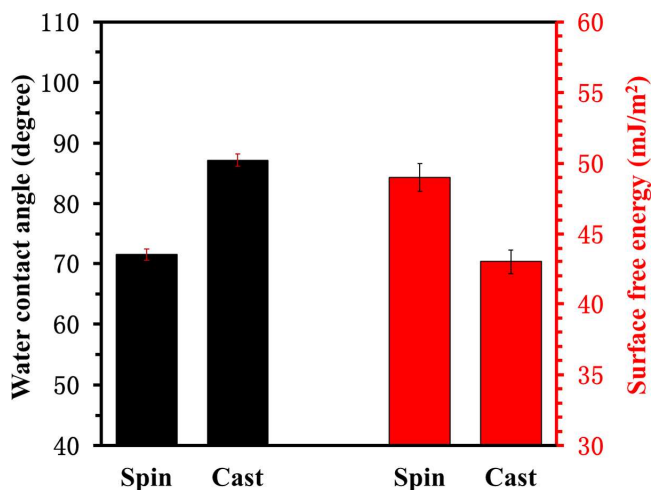


Fig.1 Water contact angle and surface free energy of PMMA films prepared by spin-coating and solution casting. The solution concentration was 2.0wt% and the spin-coating speed was 3000 rpm; $M_n=107100 \text{ g/mol}$.

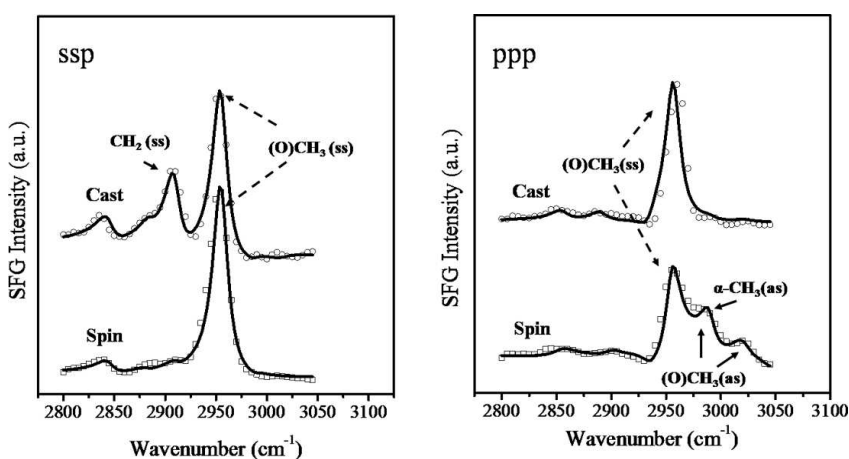


Fig. 2 SFG spectra of PMMA films prepared by spin-coating and solution casting. The solution concentration was 2.0 wt%; the spin-coating speed was 3000 rpm; $M_n=107100 \text{ g/mol}$.

Since surface wettability can be affected by roughness in addition to chemical composition, the surface graphs of both spin-coated and cast PMMA films were investigated. Fig.S1 (ESI†) shows that both film surfaces are smooth; such minimal roughness with RMS roughness below 3 nm would therefore have negligible effect on the surface wettability.³⁶ From the perspective of thermodynamics, the equilibrium state denotes the state in which the polymer chains on the film surface adopt a suitable conformation with minimum free energy. In this case, the cast PMMA film has lower free surface energy, suggesting that the polymer chains in cast films adopt a more equilibrium conformation relative to that of spin coated films. In order to obtain an insight into the wetting behavior of the film surface, the molecular structure of the outermost surface was investigated by surface-sensitive vibrational sum frequency generation (SFG) spectroscopy, which has emerged as a powerful tool for the study of the molecular structure of polymer surfaces.^{37,38} Fig. 2 shows SFG spectra over the wavenumber region from 2800 to 3050 cm^{-1} , with an *ssp* and *ppp* polarization combination, for spin-coated and cast PMMA films under ambient conditions. The peak assignments for vibrational signals of PMMA have been extensively studied. As detailed in the literature³⁷⁻⁴¹ with regard to the *ssp* SFG spectra of PMMA film, there are two major bands at 2910 and 2955 cm^{-1} , which can be assigned to the C-H symmetric stretching vibrations of the methylene groups (CH_2) in the main chain and the ester methyl groups (OCH_3), respectively. In the *ppp* SFG spectra of PMMA, the major band at around 2960 cm^{-1} is attributed to the C-H symmetric stretching vibrations of the ester methyl groups. The shoulder peak at 2990 cm^{-1} involves the C-H asymmetric stretching vibrations of the α methyl and ester methyl groups, and the 3020 cm^{-1} peak arises from the C-H asymmetric stretch of the ester methyl groups. Similar to observations reported by Tanaka⁴⁰ on cast PMMA film surfaces, hydrophobic functional moieties such as methylene groups, were present. While the α methyl group was oriented along the direction parallel to the interface, the ester methyl and methylene groups were oriented normal to the interface. Interestingly, the 2910 cm^{-1} methylene C-H symmetric stretch disappeared,

while both peaks at 2990 cm^{-1} and 3020 cm^{-1} appeared on the spin-coated PMMA film surface. This indicates that the methylene groups became randomly oriented at the spin-coated film surface or, in part, migrated into the internal region. Hydrophobic methylene groups in the main chain partially oriented in the plane of the surface with a relatively close-packed and well-ordered structure, which was in favor of decreasing the free energy. This observation is also in good agreement with both the contact angle and surface free energy of the PMMA films.

3.2 Effect of the concentration of casting solutions and molecular weight of PMMA on the surface structure of cast PMMA films

In order to correlate the relationship between the concentration of casting solution and the surface structure of the corresponding cast films, a series of casting solutions with various concentrations was utilized. Fig. 3 shows the solution concentration dependence of water contact angle of the cast films. It was observed that the water contact angle increased from 81° to 91° with increasing concentration

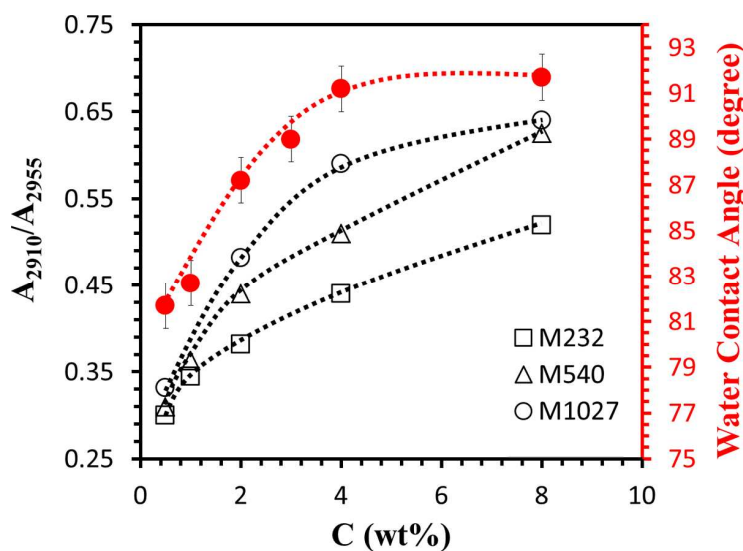


Fig.3 Concentration dependence of water contact angle (●, red) of M1027 films and A_{2910}/A_{2955} from SFG spectra of PMMA films with various molecular weights prepared by solution casting. The dashed line is a visual guide.

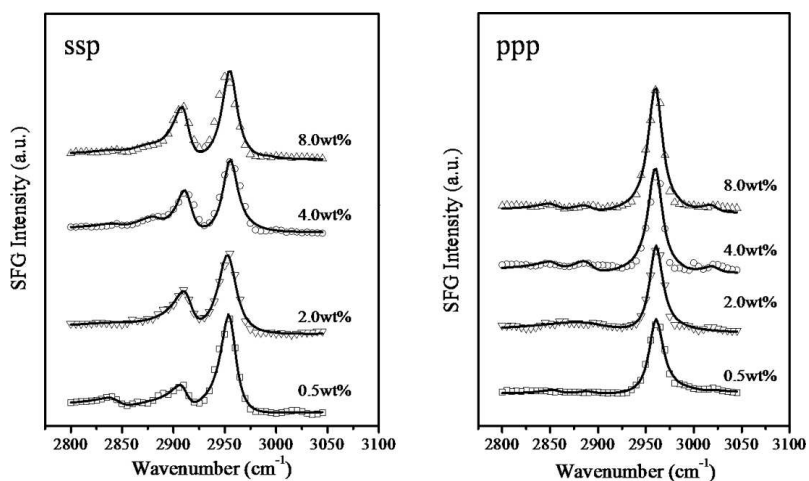


Fig. 4 SFG spectra of cast M1027 films prepared by various concentrations of casting solution. $M_n=107100$ g/mol.

of casting solution from 0.5wt% to 4wt%. The contact angle reached a constant value of 91° , when the concentration of casting solution was above 4wt%.

Fig.4 shows SFG spectra of cast PMMA films prepared by various concentrations of casting solution. It was observed that for the *ssp* spectra, the intensity of the peak at 2910 cm^{-1} increased with increasing the concentration of the film-formation solution from 0.5wt% to 4.0wt%. However, for *ppp* spectra, the intensity of the peak at 2960 cm^{-1} was not sensitive to the concentration of the casting solution. This indicates that hydrophobic methylene groups in the main chain become more closely-packed and well-ordered, oriented in the plane of the surface, with increasing the polymer concentration, while orientation of the ester methyl on the film surface changed very little.

The ratio of the peak intensity in SFG spectra from various chemical groups can be employed to reveal the fraction of chemical composition at the surface.⁴²⁻⁴⁴ At the same time, the ratio of C-H symmetric stretching vibrations of methylene to that of methyl groups as a function of temperature, which can reflect the change of the group conformation, has been used to detect the surface glass transition behavior of polypropylene⁴⁵ and poly(methyl methacrylate)⁴⁶ surfaces. Therefore, the ratio of the

C-H symmetric stretching vibrations of the methylene group (the peak at 2910 cm^{-1}) to that of ester methyl groups (the peak at 2955 cm^{-1}) in the *ssp* SFG spectra on PMMA film surfaces, A_{2910}/A_{2955} , was used as a parameter to evaluate the surface structure on the PMMA films. It is apparent in Fig. 3 that A_{2910}/A_{2955} on the cast M1027 films surfaces increased sharply with increasing the solution concentration until the concentration reached 4.0wt%, which is in good agreement with their corresponding water contact angle behavior. It was reported⁴⁰ that the peak at around 2908 cm^{-1} at the N_2 interface grew with increasing annealing temperature. These results demonstrate that once the segmental motion of a PMMA chain is free, hydrophobic methylene groups in the main chain partially orient in the plane of the N_2 interface to minimize the free interfacial energy. In this case, films cast from concentrated solution have higher water contact angle and A_{2910}/A_{2955} , suggesting that their molecular chains adopt a more equilibrium conformation relative to that of films cast from dilute solution. Once the solution concentration reached 4.0wt%, chain conformation on the resulting film surface is at a relative equilibrium state under such conditions.

Fig. 3 shows the concentration dependence of A_{2910}/A_{2955} on the surfaces of cast PMMA films with various molecular weights. Their SFG spectra are shown in Fig.S2 (ESI†). It was observed that A_{2910}/A_{2955} of the cast PMMA films increased with increasing the concentration of casting solution independent of their molecular weight. However, the incremental amplitude of the A_{2910}/A_{2955} ratio on the cast PMMA films was related to the PMMA molecular weight, which increased slowly with the concentration, since its molecular weight was relatively low. These results indicate the ease by which PMMA with high molecular weight can achieve a relative equilibrium state at the film surface, namely, forming a structure with relatively low surface free energy in which hydrophobic methylene groups in the main chain are more closely packed and have a well-ordered orientation in the plane of the surface.

3.3 Effect of solution concentration, spin-coating speed and molecular weight on the surface structure of spin-coated PMMA films

Fig. 5 shows the concentration dependence of the water contact angle of spin-coated M1027 films. The results show that the water contact angles of spin-coated M1027 films are almost independent of solution concentration when the concentration is lower than 3 wt%, and sharply increase from $\sim 72^\circ$ to $\sim 92^\circ$ when the concentration increases from 3 wt% to 8 wt%, and is then constant at $\sim 92^\circ$ as the concentration exceeds 8 wt%. It is obvious that the concentration dependence of water contact angles on the spin-coated PMMA films have a different form compared with the corresponding cast films, as shown in Fig. 3. The region of concentration within which the water contact angle increased for the cast films was 0.5 wt%-4 wt%, while that for the spin-coated film was 3 wt %-8 wt%.

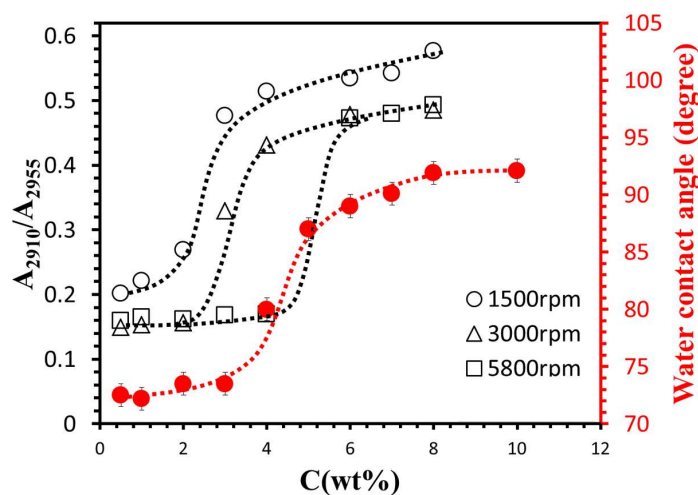


Fig. 5 Concentration dependence of water contact angle (●, red) of spin-coated M1027 films prepared at 1500 rpm and A_{2910}/A_{2955} ratio of M1027 films spin-coated at 1500 rpm (○, black), 3000rpm (△, black), 5800 rpm (□, black) . The dashed line is a visual guide.

The SFG spectra of the M1027 films spin-coated at 1500 rpm with various solution concentrations are shown in Fig. 6. All of the *ssp* SFG spectra are dominated by C-H symmetric stretching vibrations of the ester methyl groups at 2955cm^{-1} , while the CH_2 vibrational peaks at 2910cm^{-1} appear clearly on the M1027 film prepared by 2.0wt% polymer solution and then increase with the corresponding solution concentration. In the *ppp* polarization combination, the peaks at around 2990cm^{-1} and

3020cm^{-1} disappear when the concentration is higher than $3.0\text{wt}\%$. A similar trend was also found for the PMMA films spin-coated at 3000 rpm as shown in Fig. S3 (ESI†). The relationship between the A_{2910}/A_{2955} ratio of M1027 films spin-coated at 1500 rpm and corresponding concentrations of polymer solutions is shown in Fig. 5. It was found that A_{2910}/A_{2955} ratio of spin-coated M1027 film increased with increase of the solution concentration from $1.0\text{ wt}\%$ to $4.0\text{ wt}\%$ and maintained an almost constant value of 0.52 when the concentration of casting solution was up to $8\text{ wt}\%$.

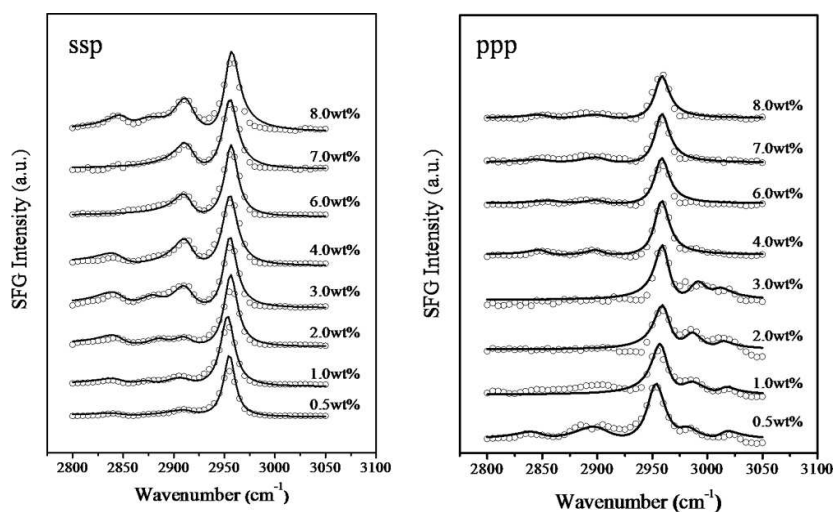


Fig.6 SFG spectra of the M1027 films spin-coated at 1500 rpm with various solution concentrations.

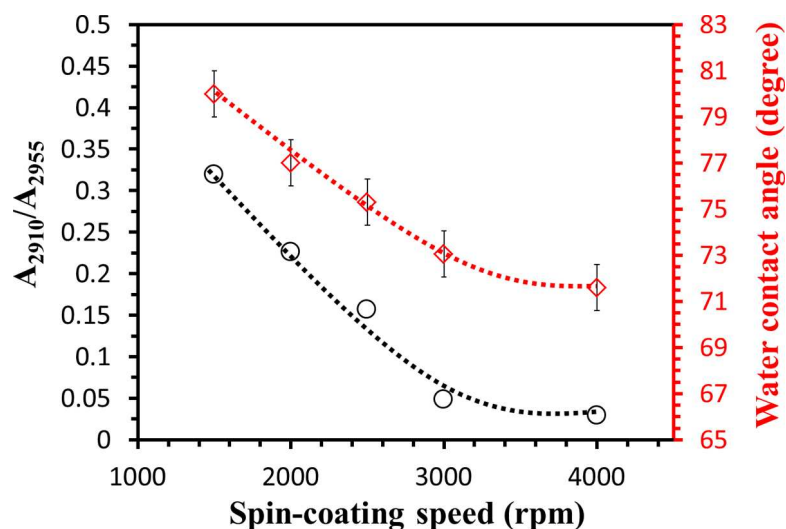


Fig. 7 $A_{2910\text{cm}^{-1}}/A_{2955\text{cm}^{-1}}$ ratio (black) and water contact angle (red) of spin-coated M1027 films as a function of spin-coating speed. The solution concentration was $4\text{ wt}\%$.

The effects of spin-coating rate on the surface structure and wettability of spin-coated PMMA films were also investigated. The results presented in Fig. 7 show that the water contact angle of M1027 films decreased from about 80° to 72° with increasing spin-coating rate from 1500 rpm to 4000 rpm. The SFG spectra of spin-coated M1027 films in Fig. 8 show that the intensity of the peak at 2910 cm^{-1} in

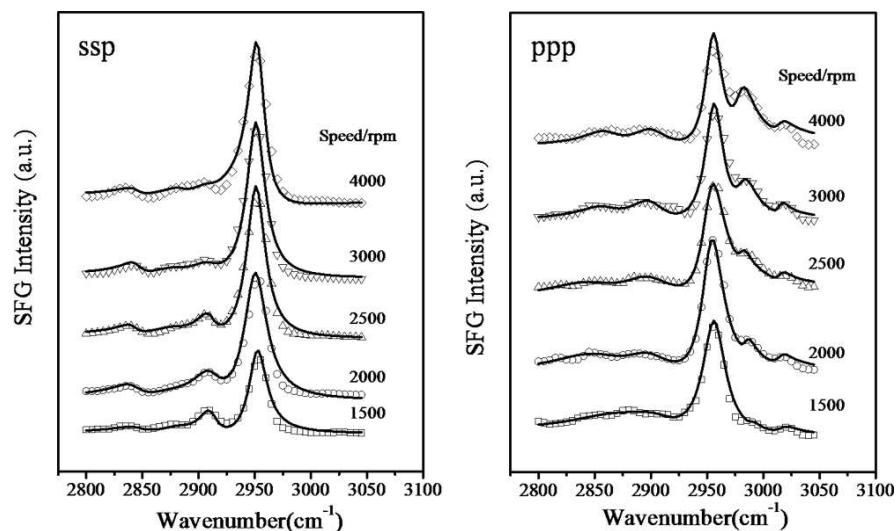


Fig. 8 SFG spectra of M1027 film spin-coated at various spin-coating rates. The concentration of casting solution was 4wt%.

ssp polarization combination decreased, while the intensities of the peaks at 2990 cm^{-1} and 3020 cm^{-1} in *ppp* polarization combination increased with increasing spin-coating speed. Similar to the water contact angle, the A_{2910}/A_{2955} ratio shown in Fig. 7 decreased with increase of the spin-coating speed.

Fig. 5 shows the concentration dependence of the A_{2910}/A_{2955} ratio of M1027 films spin-coated at various spin-coating speeds. Two break points are evident in each curve. The A_{2910}/A_{2955} ratio of spin-coated M1027 films remains at an almost constant value of 0.18 in the low concentration region of polymer solution. After this plateau region, the A_{2910}/A_{2955} ratio increases sharply with increase of the corresponding concentration of the solution. After the concentration approaches a certain value, the A_{2910}/A_{2955} ratio of the corresponding spin-coated M1027 films remains almost

constant as the solution concentration increases. The solution concentration corresponding to the offset point of the curves shifts to higher value when the spin-coating speed is enhanced. The concentration region of polymer solution, within which the A_{2910}/A_{2955} ratio of spin-coated M1027 films increased sharply, was 1-3wt%, 2-4wt% and 4-6wt%, corresponding to spin-coating rates of 1500rpm, 3000rpm and 5800rpm respectively. The A_{2910}/A_{2955} ratios of spin-coated PMMA films with different molecular weight as a function of the solution concentration are shown in Fig.S4 (ESI†). It is apparent that the A_{2910}/A_{2955} ratio of the spin-coated films is related to both solution concentration and PMMA molecular weight. Within the range of investigated concentrations, the A_{2910}/A_{2955} ratios of spin-coated PMMA films with higher molecular weight increased more quickly with the solution concentration compared with PMMA films with relatively low molecular weight.

The results above indicate that the surface structure of spin-coated PMMA films was close to that of the cast films when the spin-coating rate was low, in which the hydrophobic methylene groups in the main chain were oriented in the plane of the surface with a more closely-packed and well-ordered structure. When the high spin-coating rate was applied, the higher concentration of polymer solution was necessary for the corresponding spin-coated film to adopt a more equilibrium conformation. At the same time, it was observed that the surface structure of spin-coated PMMA films with high molecular weight exhibited a relative equilibrium state compared with that of the corresponding film with relatively low molecular weight, even though its surface structure was still far from that of the solution casting films. In addition, the surface structure of the spin-coated PMMA films was affected greatly by its molecular weight compared with that of the cast film.

3.4 The cause of solution concentration and molecular weight dependence of surface structure of PMMA films

It is commonly observed that polymer chains tend to form aggregates in polymer solutions of sufficiently high concentration.⁴⁷ The origin of the aggregation is the interchain attraction forces. Since these interactions are short-range forces, the

polymer chains are isolated in dilute solution, thus these intermolecular forces can be neglected. It is expected that the probability for the coiled polymer chains to penetrate into each other is small. As the concentration increases and the distance between the polymer chains decreases, these interchain forces become more significant. As a result, the polymer coils start to entangle with each other to form “loose aggregates”. It is predicated that further increases in the concentration will eventually result in heavy interpenetration of the polymer chains, or the formation of “strong aggregation”. From this point of view, one would expect that these interactions are maximized in the solid state when the polymer chains are densely packed. In fact, the formation of aggregates in thin films is well-documented for various polymers.

From the above discussion, one would expect that the structure of a spin-coated film depends on the relative strengths of the cohesive force of the solution and the centrifugal force asserted by the spinning. When the centrifugal force is comparable to the cohesive force of the solution, one would expect to see a spinning speed dependence of the film morphology. In this regard, the viscosity of the polymer solution can, to a certain extent, reflect the intermolecular interactions. Although other factors such as the coil size and topology of polymer also affect the viscosity of the solution, it was reasonable that the intermolecular force was main factor to affect

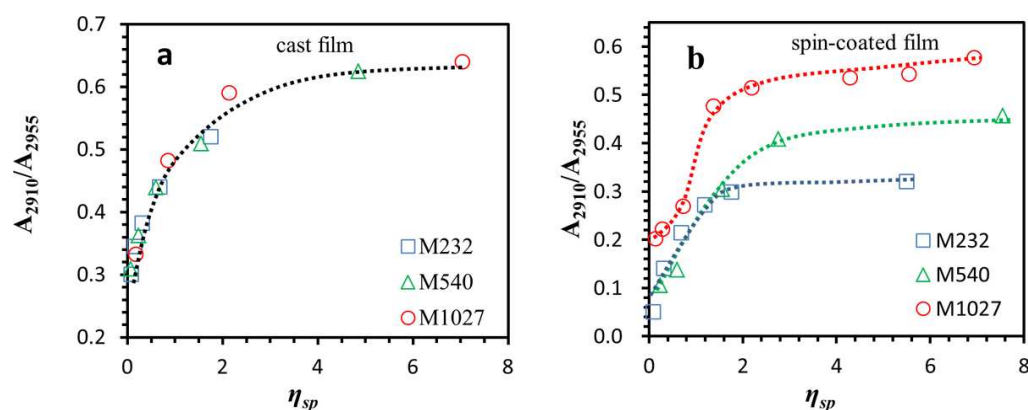


Fig. 9 Specific viscosity dependence of A_{2910}/A_{2955} ratio of cast (a) and spin-coated PMMA films (b) with different molecular weights. The spin-coated PMMA films were prepared using a 1500 rpm spin-coating rate. The dashed line is a visual guide.

solution viscosity. In other words, a higher solution viscosity suggests higher intermolecular forces, and *vice versa*.^{47,48} Fig. S5 (ESI†) shows the plot of the specific viscosity, η_{sp} of the solution versus the polymer concentration. It is apparent that η_{sp} is related to both the solution concentration and the corresponding molecular weight of PMMA. When the solution concentration is the same, the PMMA solution with the higher molecular weight has a relatively high η_{sp} . The specific viscosity dependence of A_{2910}/A_{2955} of both cast and spin-coated PMMA films with different molecular weights is presented in Fig. 9. It may be observed that the A_{2910}/A_{2955} ratio for both cast and spin-coated PMMA films increased with increasing η_{sp} of the corresponding polymer solution. However, the surface structure dependence of viscosity in the film-formation solutions exhibited different characteristics, according to the specific film-formation method. The A_{2910}/A_{2955} ratio of cast PMMA films increased with η_{sp} of the corresponding solution, while no molecular weight dependence was found (Fig.9a). For the spin-coated PMMA films, their surface structure was affected by both viscosity of film-formation solution and polymer molecular weight (Fig.9b).

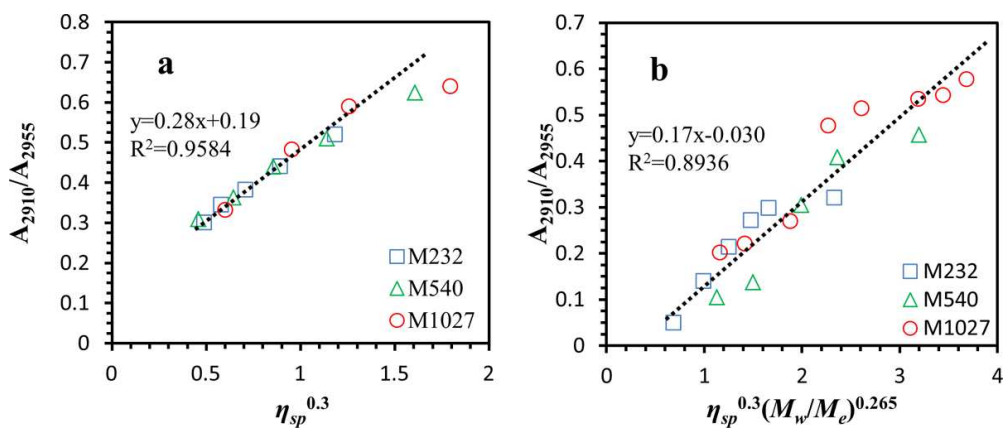


Fig. 10 A_{2910}/A_{2955} ratio of cast (a) and spin-coated (b) PMMA films vs η_{sp} of film-formation solution and their M_w/M_e . The spin-coated PMMA films were prepared using a 1500 rpm spin-coating rate.

Taking the molecular weight into consideration, the quantitative correlation among A_{2910}/A_{2955} , the specific viscosity η_{sp} and M_w/M_e are shown in Fig. 10. The results clearly show that the A_{2910}/A_{2955} ratios of cast PMMA films have a linear relationship with $\eta_{sp}^{0.3}$ of the corresponding polymer solutions, while the A_{2910}/A_{2955} ratios of spin-coated PMMA films have a linear relationship with $\eta_{sp}^{0.3}(M_w/M_e)^{0.26}$, in which $M_e = 7000\text{g/mol}$ as reported.⁴⁹ With regard to the origin of these interesting phenomena, we have to consider the conformation, degree of entanglement or the aggregation state of the polymer chains in the precursor solution and the film-forming process during spin-coating and solution casting. On one hand, the polymer chains tend to adopt different conformation states in solutions with different concentrations. Based on the literature^{50,51}, the concentration dependence of the specific viscosity of polymer solutions can be divided into three regions: (1) When the solutions are dilute, the macromolecular chains are separated and cannot make contact with each other; thus the viscosity of the polymer solution is small. (2) When the solutions are semi-dilute, the dimensions of the macromolecular chains decrease and they contact each other due to the thermal motion. The quantity of isolated chains is reduced and a certain amount of entanglement occurs, so that the degree of chain entanglement increases and large systems of entangled chains are formed, resulting in viscosity increasing sharply with increasing concentration. (3) When the solutions are concentrated, the density of chain entanglement still increases with increasing concentration, but the variation in the degree of entanglement is small. Thus, by comparison, it may be inferred from the above that the surface structure of the resulting PMMA film is related to the entanglement of the PMMA chains in the corresponding casting solution.

It was accepted that when a film was prepared by polymer solution casting, the polymer concentration in the film increased as the solvent evaporated during film-formation.^{52,53} In thermal equilibrium, the number of entanglements per chain with surrounding chains increases with polymer concentration. The entanglement density will be enhanced further by annealing the polymer film. The re-entanglement of the chains in the film by annealing was found to be substantially longer than the

reputation time.⁵² As a result, some memory of the chain conformations in the solution may carry over to the resulting dry film, including that of its surface. A higher degree of PMMA chain entanglement on the film surface was obtained when the film was prepared using a relatively high concentration of casting solution, which was related to its viscosity.⁵⁴ Solution-casting is a relatively mild process during which the solvent evaporates slowly, allowing enough time for the polymer chains to minimize free energy by adjusting their chain conformation. As the solution concentration increases, the polymer chains will penetrate and entangle with each other, contributing to achieve equilibrium state. When the concentration of casting solution is relatively high, the density of chain entanglement in the solution is increased, resulting in higher viscosity. The relative equilibrium state on a film surface is easily achieved when casting solution with relative high viscosity is employed to prepare PMMA film by solution casting. Therefore, the $A_{2910\text{cm}^{-1}}/A_{2955\text{cm}^{-1}}$ ratio of cast PMMA films has a linear relationship with $\eta_{sp}^{0.3}$ of corresponding casting PMMA solution, independent of the PMMA molecular weight.

In 1952 Bueche⁵⁵ proposed the first model for the extra frictional drag conferred by entanglement interactions and used it to calculate the molecular weight dependence of melt viscosity for linear chains. The result was $\eta_o \propto M^{3.5}$ for highly entangled chains, in good agreement with the empirical relation, found at high molecular weights. It was suggested by Bueche⁵⁶ that viscosity behavior above M_c , where M_c is a certain molecular weight which is two or three times larger than M_e , can be explained simply in terms of an enhanced Stoke friction for the molecules. Bueche^{55,57} further suggested that since polymer molecules in concentrated systems are looped through the coils of neighboring molecules, relative motion must be resisted by the need for these loops to slip around one another. Each molecule is assumed to participate in an average of E such temporary couples, creating a temporary network of Gaussian segments joining $vE/2$ couples per unit volume. The coupling frequency is taken to be proportional to the corresponding molecular weight. E is the average number of entanglement points per molecule ($E = M_w/M_e$). In

concentrated solutions, $E \propto cM$, assuming entanglement coupling to be simply a special kind of segment-segment contact. Spin-coating is a much more vigorous process than the solution-casting method, and at least two factors should be taken into account: (1) The rapid solvent evaporation during spin-coating results in a lowered entanglement density, allowing the polymer chains to have much less time to adjust their conformation. (2) The centrifugal force during spin-coating can induce the polymer chains to be extended. These two factors result in forming a more non-equilibrium structure compared with the films prepared by the solution-casting method.

Accumulating experimental evidence shows that the shearing field caused by a high spin-coating speed has a great influence on the orientation of polymer chains.^{4,58,59} Therefore, the relative strength of the cohesive force of the solution and the centrifugal force asserted by spin-coating determine the chain conformation or the aggregation state of a spin-coated film. It was accepted that the extra frictional drag conferred by entangling interactions will increase with increasing E ($E = M/M_e$), resulting in high viscosity for the polymer with high molecular weight. The entangled polymer chains in solution with higher E will be more difficult to stretch, and accordingly be deformed by centrifugal force during spin-coating. The relative equilibrium state on the resulting film surface is therefore easily obtained. Thus, the surface structures (A_{2910}/A_{2955}) of spin-coated PMMA films have a linear relationship with $\eta_{sp}^{0.3} E^{0.26}$, namely $\eta_{sp}^{0.3} (M_w/M_e)^{0.26}$, as shown in Figure 10. Since the centrifugal force increased with increasing spin-coating rate, the concentration of casting solution which could attain a certain entanglement density of chains on the resulting film surface was enhanced. Therefore, the concentration region of polymer solution, within which the A_{2910}/A_{2955} ratio of corresponding spin-coated films started increasing sharply, was 1-3wt%, 2-4wt% and 4-6wt%, corresponding to spin-coating rates of 1500 rpm, 3000 rpm and 5800 rpm respectively, as shown in Figure 5.

4. CONCLUSIONS

The effects of properties of film-formation solution on the corresponding surface structure of poly(methyl methacrylate) (PMMA) films were systematically investigated by contact angle goniometry and sum-frequency generation spectroscopy (SFG). It was observed that the water contact angles on both spin-coated and cast films increased with increasing concentration of casting solution. Compared with spin-coated films, it was apparent that the corresponding cast PMMA films had a relatively high water contact angle and lower surface free energy, indicating that the polymer chains on the surface of cast PMMA films adopted a relative equilibrium conformation from the perspective of thermodynamics. This was confirmed by the SFG measurements. It was observed that the intensity of the peak at 2910 cm^{-1} , attributed to the C-H symmetric stretching vibrations of the methylene groups (CH_2) in the main chain, increased with increasing the concentration of film-formation solution, which suggests that hydrophobic methylene groups partially oriented in the plane of the surface with a relatively close-packed and well-ordered structure, resulting in a decrease of the surface free energy. The ratio of C-H symmetric stretching vibrations of methylene groups (the peak at 2910 cm^{-1}) to that of ester methyl groups (the peak at 2955 cm^{-1}) from SFG spectra, A_{2910}/A_{2955} , was used as a parameter to evaluate the structure on the film surface, which was related to wettability of the film surface. The results showed that A_{2910}/A_{2955} ratio of cast PMMA films increased linearly with $\eta_{sp}^{0.3}$ (η_{sp} , the specific viscosity of the casting solution), whereas that of the corresponding spin-coated films exhibited a linear relationship with $\eta_{sp}^{0.3}E^{0.26}$ in which E was the average number of entanglement points per molecule ($E=M_w/M_e$). The reason for this observed difference in A_{2910}/A_{2955} ratio dependence on specific viscosity may be attributed to chain entanglement in the corresponding polymer solution. A relative equilibrium conformation on the PMMA film surface, adopted from the perspective of thermodynamics, was easily achieved during film formation when the conformation of polymer chain in corresponding casting solution was close to that in the bulk. For the spin-coated films, the chain

entanglement structure in the casting solution was a more important factor for the resulting film to reach a relative equilibrium state, since this structure could inhibit the deformation of polymer chain during spin-coating.

This work may help to enhance the fundamental understanding of the formation of film surface structure development from polymer solution to the resulting solid film, which will affect not only the corresponding surface properties, but also the dynamics of the resulting thin films.

Acknowledgements

We are thankful for support from the National Natural Science Foundation of China (NSFC, No.21174134, No.21374104) and the Natural Science Foundation of Zhejiang Province (No. LY13B040005).

Notes

Department of Chemistry, Key Laboratory of Advanced Textile Materials and Manufacturing Technology of the Education Ministry, Zhejiang Sci-Tech University, Hangzhou 310018, China.

* Email: wxinping@yahoo.com or wxinping@zstu.edu.cn . Tel/fax: +86-571-8684-3600.

Supplementary Information

† Electronic Supplementary Information (ESI) available: AFM topographies of both cast and spin-coated PMMA films; SFG spectra of cast M540 films prepared by various concentrations; SFG spectra of M1027 films spin-coated at 3000rpm by

various concentrations; A_{2910}/A_{2955} of spin-coated PMMA films with different molecular weights as a function of the solution concentration; relationship between the specific viscosity and solution concentration. See DOI: 10.1039/b000000x/

References

- 1 M. Stamm, *Polymer Surfaces and Interfaces: Characterization, Modification, and Applications*, Springer-Verlag, Berlin and Heidelberg, Germany, 2008.
- 2 G. H. Lu, L. G. Li, S. J. Li, Y. P. Qu, H. W. Tang and X. N. Yang, *Langmuir*, 2009, **25**, 3763–3768.
- 3 H. E. Schaefer, *Nanoscience: The Science of the Small in Physics, Engineering, Chemistry, Biology and Medicine*, Springer-Verlag, Berlin and Heidelberg, Germany, 2010.
- 4 C. W. Y. Law, K. S. Wong, Z. Yang, L. E. Horsburgh and A. P. Monkman, *Appl. Phys. Lett.*, 2000, **76**, 1416–1418.
- 5 D. B. Hall, P. Underhill and J. M. Torkelson, *Polymer Engineering and Science*, 1998, **38**, 2039–2945.
- 6 W. W. Flack, D. S. Soong, A. T. Bell and D. W. Hess, *J. Appl. Phys.*, 1984, **56**, 1199–1206.
- 7 Y. Urushihara and T. Nishino, *Langmuir*, 2005, **21**, 2614–2618.
- 8 B. Zuo, W. L. Liu, H. Fan, Y. Z. Zhang, T. T. He and X. P. Wang, *Soft Matter*, 2013, **9**, 5428–5437.
- 9 K. Shuto, Y. Oishi, T. Kajiyama and C. C. Han, *Macromolecules*, 1993, **26**, 6589–6594.
- 10 R. L. Jones, S. K. Kumar, D. L. Ho, R. M. Briber and T. P. Russell, *Nature*, 1999, **400**, 146–149.
- 11 H. G. Ni, X. H. Li, Y. Y. Hu, B. Zuo, Z. L. Zhao, J. P. Yang, D. X. Yuan, X. Y. Ye and X. P. Wang, *J. Phys. Chem. C*, 2012, **116**, 24151–24160.
- 12 A. Brulet, F. Boue, A. Menelle and J. P. Cotton, *Macromolecules*, 2000, **33**, 997–1001.

- 13 Z. H. Yan, R. P. Zhang, Y. R. Zhao, B. Zuo, F. F. Zheng, T. Y. Chen, X. P. Wang and Z. Q. Shen, *Sci. China. Ser. B-Chem.*, 2012, **55**, 1263–1273.
- 14 Y. L. Hei, M. Deng, X. Y. Ye, H.G. Ni, P. Ye, X. P. Wang, Z. Q. Shen, *Sci. China. Ser. B-Chem.*, 2009, **39**, 1627–1637.
- 15 X. H. Zhang, J. F. Douglas and R. L. Jones, *Soft Matter*, 2012, **8**, 4980–4987.
- 16 X. L. Lu and Y. L. Mi, *Macromolecules*, 2005, **38**, 839–843.
- 17 H. Tsuruta, Y. Fujii, N. Kai, H. Kataoka, T. Ishizone, M. Doi, H. Morita and K. Tanaka. *Macromolecules*, 2012, **45**, 4643–4649.
- 18 X. L. Lu, I. Cheng and Y. L. Mi, *Polymer*, 2007, **48**, 682–686.
- 19 Y. Shi, J. Liu and Y. Yang, *J. Appl. Phys.*, 2000, **87**, 4254–4263.
- 20 M. Kobashi and H. Takeuchi. *Macromolecules*, 1998, **31**, 7273–7278.
- 21 L. Y. Wong, R. Q. Png, F. B. Shanjeera Silva, L. L. Chua, D. V. Maheswar Repaka, S. Chen, X. Gao, L. Ke, S. J. Chua, A. T. S. Wee and P. K. H. Ho. *Langmuir*, 2010, **26**, 15494–15507.
- 22 A. M. Botelho do Rego, O. Pellegrino, J. M. G. Martinho and J. Lopes da Silva, *Langmuir*, 2000, **16**, 2385–2388.
- 23 X. Y. Ye, B. Zuo, M. Deng, Y. L. Hei, H. G. Ni, X. L. Lu and X. P. Wang, *J. Colloid Interface Sci.*, 2010, **349**, 205–214.
- 24 D. W. Xue, X. P. Wang, H. G. Ni, W. Zhang and G. Xue. *Langmuir*, 2009, **25**, 2248–2257.
- 25 J. L. Keddie, R. A. L. Jones and R. A. Cory, *Europhys Lett.*, 1994, **27**, 59–64.
- 26 J. A. Forrest and J. Mattsson, *Phys. Rev. E: Stat., Nonlinear, Soft Matter Phys.*, 2000, **61**, 53–56.
- 27 J. P. Yang, D. X. Yuan, B. Zhou, J. Gao, H. G. Ni, L. Zhang and X. P. Wang, *J. Colloid Interface Sci.*, 2011, **359**, 269–278.
- 28 X. F. Wang, H. G. Ni, D. W. Xue, X. P. Wang, R. R. Feng and H. F. Wang, *J. Colloid Interface Sci.*, 2008, **321**, 373–383.
- 29 D. K. Owens and R. C. Wendt, *J. Appl. Polym. Sci.*, 1969, **13**, 1741–1747.
- 30 Y. R. Shen, *The Principles of Nonlinear Optics*, Wiley-Interscience, New York, 1984.

- 31 X. L. Lu, G. Xue, X. P. Wang, J. L. Han, X. F. Han, J. Hankett, D. W. Li and Z. Chen, *Macromolecules*, 2012, **45**, 6087–6094.
- 32 B. Zuo, Y. Y. Hu, X. L. Lu, S. X. Zhang, H. Fan and X. P. Wang, *J. Phys. Chem. C.*, 2013, **117**, 3396–3406.
- 33 Q. Du, R. Superfine, E. Freysz and Y. R. Shen, *Phys. Rev. Lett.*, 1993, **70**, 2313–2316.
- 34 K. G. Tingey and J. D. Andrade, *Langmuir*, 1991, **7**, 2471–2478..
- 35 X. P. Wang, X. B. Wang and Z. F. Chen, *Polymer*, 2007, **48**, 522–529.
- 36 Wu, S. *Polymer Interface and Adhesion*, Marcel Dekker, New York, 1982.
- 37 J. Wang, C. Y. Chen, S. M. Buck and Z. Chen, *J. Phys. Chem. B*, 2001, **105**, 12118–12125.
- 38 M. L. Clarke, C. Y. Chen, J. Wang and Z. Chen, *Langmuir*, 2006, **22**, 8800–8806.
- 39 K. C. Jena, P. A. Covert, S. A. Hall and D. K. Hore, *J. Phys. Chem. C*, 2011, **115**, 15570–15574.
- 40 Y. Tateishi, N. Kai, H. Noguchi, K. Uosaki, T. Nagamura and K. Tanaka, *Polym. Chem.*, 2010, **1**, 303–311.
- 41 A. Horinouchi, H. Atarashi, Y. Fujii and K. Tanaka, *Macromolecules*, 2012, **45**, 4638–4642.
- 42 E. Amitay-Sodavsky, K. Komvopoulos, Y. Tian and G. A. Somorjai, *Appl. Phys. Lett.*, 2002, **80**, 1829–1831.
- 43 E. Amitay-Sodavsky, K. Komvopoulos, R. Ward and G. A. Somorjai, *Appl. Phys. Lett.*, 2003, **83**, 3066–3068.
- 44 H. K. Ye, A. Abu-Akeel, J. Huang, H. E. Katz and D. H. Gracias, *J. Am. Chem. Soc.*, 2006, **128**, 6528–6529.
- 45 D. H. Gracias, D. Zhang, L. Lianos, W. Ibach, Y. R. Shen and G. A. Somorjai, *Chem. Phys.*, 1999, **245**, 277–284.
- 46 B. Zuo, Y. J. Liu, L. Wang, Y. M. Zhu, Y. F. Wang and X. P. Wang, *Soft Matter*, 2013, **9**, 9376–9384.
- 47 E. Wyn-Jones and J. Gormally, *Aggregation Processes in Solution*, Elsevier, Amsterdam, 1983.

- 48 (a) A. Ohshima, H. Kudo, T. Sato and A. Teramoto, *Macromolecules*, 1995, **28**, 6095–6099; (b) A. Ohshima, A. Yamagata and T. Sato, *Macromolecules*, 1999, **32**, 8645–8654.
- 49 K. Fuchs, C. Friedrich and J. Weese, *Macromolecules*, 1996, **29**, 5893–5901.
- 50 R. H. Colby, L. J. Fetters, W. G. Funk and W. W. Graessley, *Macromolecules*, 1991, **24**, 3873–3882.
- 51 A. V. Dobrynin, R. H. Colby and M. Rubinstein, *Macromolecules*, 1995, **28**, 1859–1871.
- 52 D. R. Barbero and U. Steiner, *Phys. Rev. Lett.*, 2009, **102**, 248303.
- 53 K. R. Thomas, A. Chenneviere, G. Reiter and U. Steiner, *Phys. Rev. E: Stat., Nonlinear, Soft Matter Phys.*, 2011, **83**, 021804.
- 54 H. K. Tian, Y. H. Yang, J. Ding, W. L. Liu, B. Zuo, J. P. Yang and X. P. Wang, *Soft Matter*, 2014, **10**, 6347–6356.
- 55 F. Bueche, *J. Chem. Phys.*, 1952, **20**, 1959–1964.
- 56 F. Bueche, W. M. Cashin and P. Debye, *J. Chem. Phys.*, 1952, **20**, 1956–1958.
- 57 (a) F. Bueche, *J. Chem. Phys.*, 1956, **25**, 599–600. (b) F. Bueche, *J. Chem. Phys.*, 1964, **40**, 484–487.
- 58 L. L. Kosbar, S. W. J. Kuan, C. W. Frank and R. F. W. Pease, *ACS Symp. Ser.*, 1989, **381**, 95–111.
- 59 M. M. Despotopoulou, R. D. Miller, J. F. Rabolt and C. W. Frank, *J. Polym. Sci. Part B: Polym. Phys.*, 1996, **34**, 2335–2349.